

Supporting Information

Chemically Treated IGZO-based Highly Visible-Blind UV Phototransistor with Suppression of Persistent Photoconductivity Effect

*Min Gye Kim,^{a,b} Jun Hyung Jeong,^{a,b} Jin Hyun Ma,^{a,b} Min Ho Park,^{a,b} Seunghwan Kim,^c
Soohyung Park,^{c,d} and Seong Jun Kang^{a,b,*}*

^aDepartment of Advanced Materials Engineering for Information and Electronics, Kyung Hee University, Yongin 17104, Republic of Korea

^bIntegrated Education Institute for Frontier Science & Technology (BK21 Four), Kyung Hee University, Yongin 17104, Republic of Korea

^cAdvanced Analysis Center, Korea Institute of Science and Technology (KIST), Seoul 02792, Republic of Korea

^dDivision of Nano & Information Technology, KIST School, University of Science and Technology (UST), Seoul 02792, Republic of Korea

*Corresponding author: Tel: +82-31-201-3324

E-mail: junkang@khu.ac.kr (S. J. Kang)

Index

Figure S1. (a) XRD analysis of pristine IGZO and 2EEG-IGZO with a specific volume ratio of 8:1:2 and (b) FFT image of 2EEG-IGZO with 8:1:1 vol%.

Figure S2. Transfer curves (left) and SQRT drain current (I_D) curves (right, blue) versus V_G for (a) IGZO, (b-d) 2EEG-IGZO with volume ratios of 8:1:1, 8:1:2, and 8:1:4 vol%, respectively.

Figure S3. Optical bandgap energy of (a) IGZO, (b-e) 2EEG-IGZO samples with various volume ratio of 2-EE and EG (8:1:1, 8:1:2, 8:1:4, 8:1:8 vol%) calculated by Tauc plot method.

Figure S4. XPS O 1s spectra of bare IGZO sample.

Figure S5. XPS spectra of (a) In 3d, (b) Ga 2p, (c) Zn 2p for IGZO, 2EEG-IGZO samples (8:1:1, 8:1:2, 8:1:4, 8:1:8 vol%).

Figure S6. Transfer characteristics under NBS ($V_G = -20$ V) of (a) pristine IGZO and 2EEG-IGZOs with different volume ratios of (b) 8:1:1, (c) 8:1:2, (d) 8:1:4, and (e) 8:1:8, respectively. (f) V_{th} shift with stress time under NBS condition.

Figure S7. Transfer curves under NBIS ($V_G = -20$ V) of (a) pristine IGZO and 2EEG-IGZOs with different volume ratios of (b) 8:1:1, (c) 8:1:2, (d) 8:1:4, and (e) 8:1:8, respectively. (f) V_{th} shift with various stress time under NBIS condition.

Figure S8. XPS N 1s spectra of bare IGZO sample.

Figure S9. XPS C 1s spectra of (a) IGZO, 2EEG-IGZO samples with volume ratios of 8:1:1, 8:1:2, 8:1:4, 8:1:8 vol%, and (b) the four deconvoluted C 1s peak of IGZO.

Figure S10. Urbach energy plots of the IGZO, 2EEG-IGZO samples with different additive volume ratio of 8:1:1, 8:1:2, 8:1:4, and 8:1:8 vol%, respectively.

Figure S11. Photosensitivities of pristine IGZO and 2EEG-IGZO samples with varying vol% ratios (8:1:1, 8:1:2, 8:1:4, and 8:1:8) as a function of V_G , measured under red, green, blue, and UV light.

Figure S12. Contact angle measurements of IGZO and 2EEG-IGZO with various composition ratios (8:1: x).

Figure S13. XPS C 1s spectra of 2EEG-IGZO samples (8:1:1 vol% ratio) without UVO treatment and with UVO treatment durations of 1 min, 2 min, and 3 min, respectively.

Figure S14. Contact angle measurements of 2EEG-IGZO (8:1:1 vol%) with different UVO treatment duration of 1 min, 2 min, and 3 min, respectively.

Figure S15. Optical bandgap energy of 2EEG-IGZO (8:1:1 vol% ratio) with varying UVO treatment durations: (a) 1 min, (b) 2 min, and (c) 3 min, respectively.

Figure S16. Photosensitivity of 2EEG-IGZO phototransistors under red (635 nm) and green (520 nm) illumination as a function of UVO treatment time.

Figure S17. Photoresponse characteristics of 2EEG-IGZO phototransistors under red (635 nm) and green (520 nm) illumination as a function of UVO treatment time: (a) before (left) and after 1 min. UVO treatment (right), and (b) before (left) and after UVO treatment with a duration of 2 min.

Figure S18. Transfer characteristics of 2EEG-IGZO (8:1:1) under NBS condition with different UVO treatment duration of (a) 1 min, (b) 2 min, and (c) 3 min, and under NBIS condition with (d) 1 min, (e) 2 min, and (f) 3 min of UVO treatment durations, respectively. ($V_G = -20V$)

Figure S19. (a) Temporal photoresponse of 2EEG-IGZO (8:1:1 vol%) as a function of UVO treatment duration (0, 1, 2, 3 min) and (b)-(e) the corresponding rising/falling times of each sample. ($V_G = -15V$, $V_D = 0.1 V$)

Figure S20. A real outdoor experiment image to clarify the potential of optimized 2EEG-IGZO TFTs as a real UV sensor.

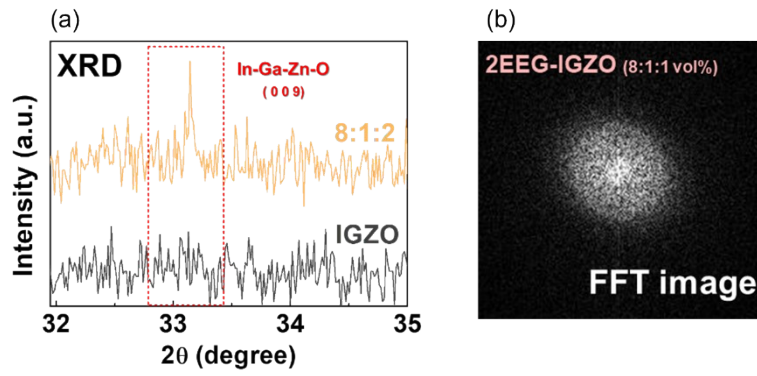


Figure S1. (a) XRD analysis of pristine IGZO and 2EEG-IGZO with a specific volume ratio of 8:1:2 and (b) FFT image of 2EEG-IGZO with 8:1:1 vol%.

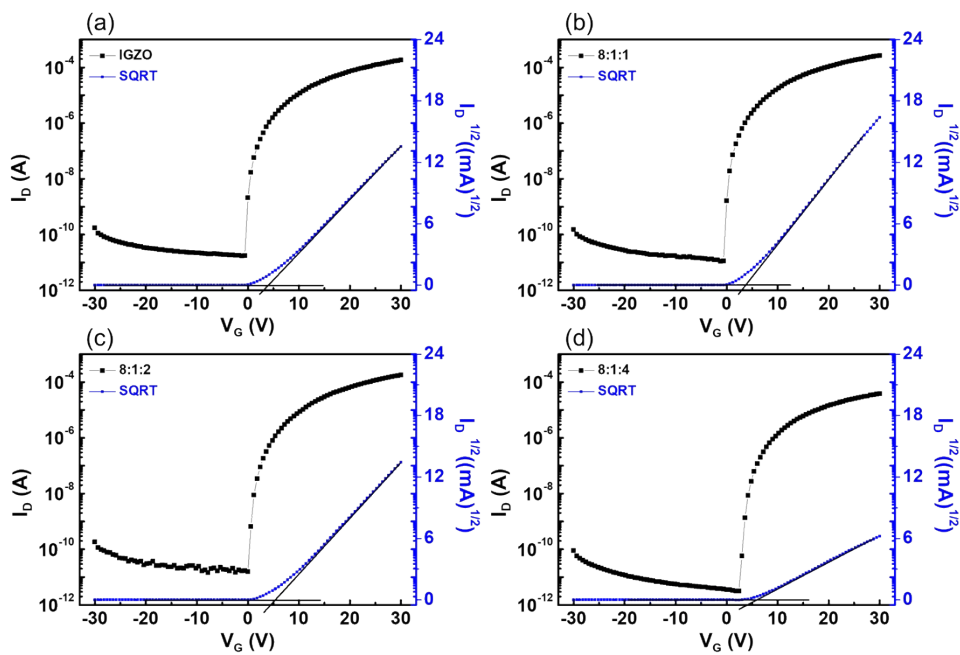


Figure S2. Transfer curves (left) and SQRT drain current (I_D) curves (right, blue) versus V_G for (a) IGZO, (b-d) 2EEG-IGZO with volume ratios of 8:1:1, 8:1:2, and 8:1:4 vol%, respectively.

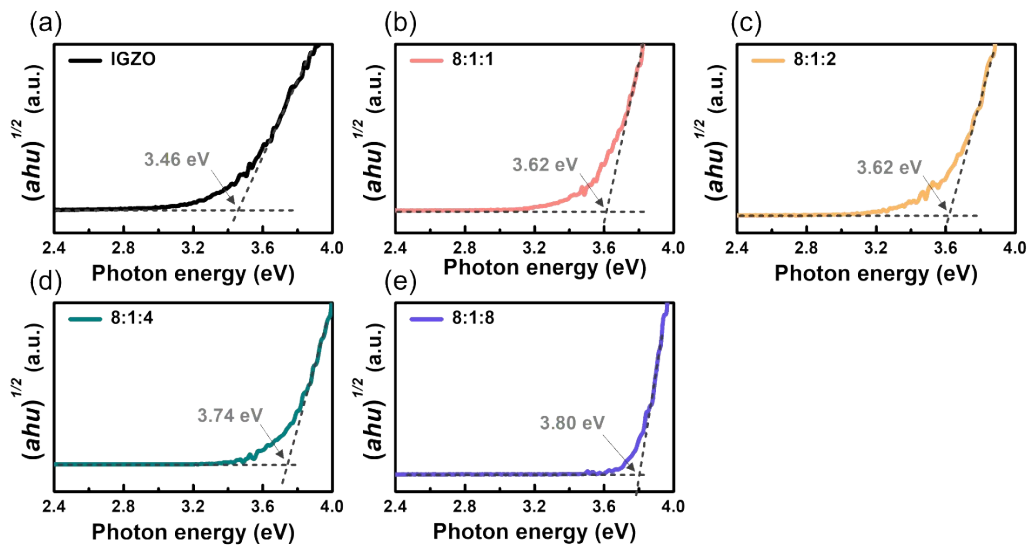


Figure S3. Optical bandgap energy of (a) IGZO, (b-e) 2EEG-IGZO samples with various volume ratio of 2-EE and EG (8:1:1, 8:1:2, 8:1:4, 8:1:8 vol%) calculated by Tauc plot method.

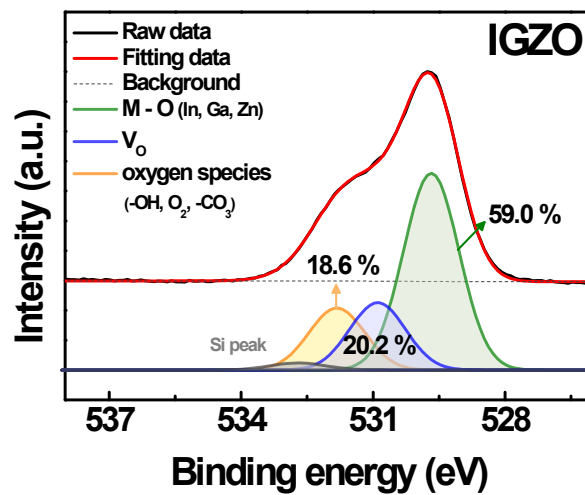


Figure S4. XPS O 1s spectra of bare IGZO sample.

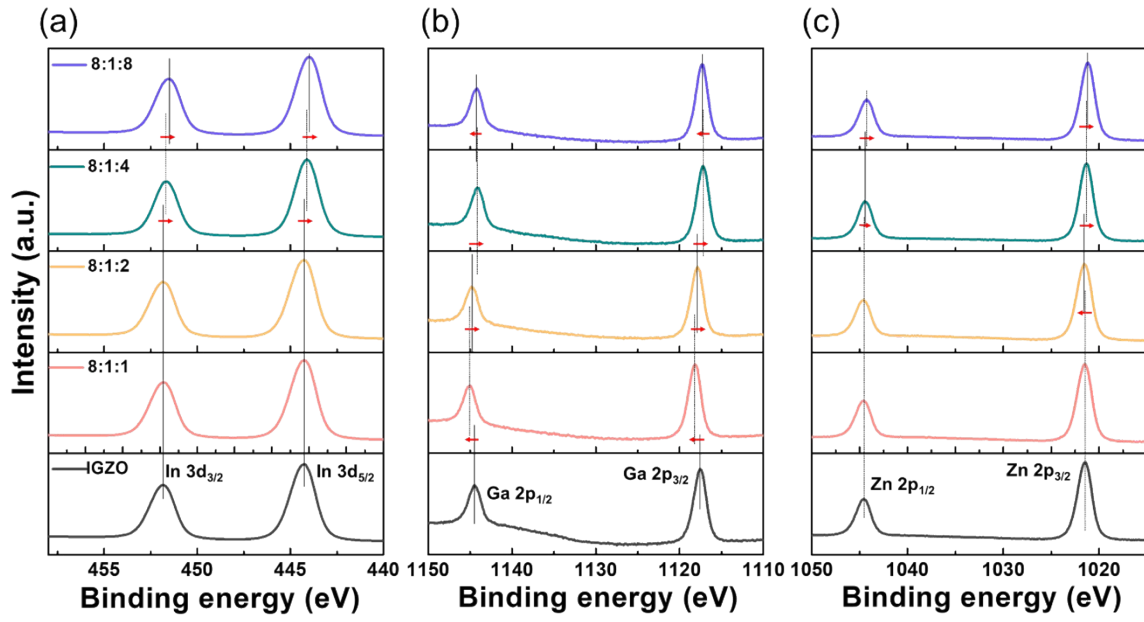


Figure S5. XPS spectra of (a) In 3d, (b) Ga 2p, (c) Zn 2p for IGZO, 2EEG-IGZO samples (8:1:1, 8:1:2, 8:1:4, 8:1:8 vol%).

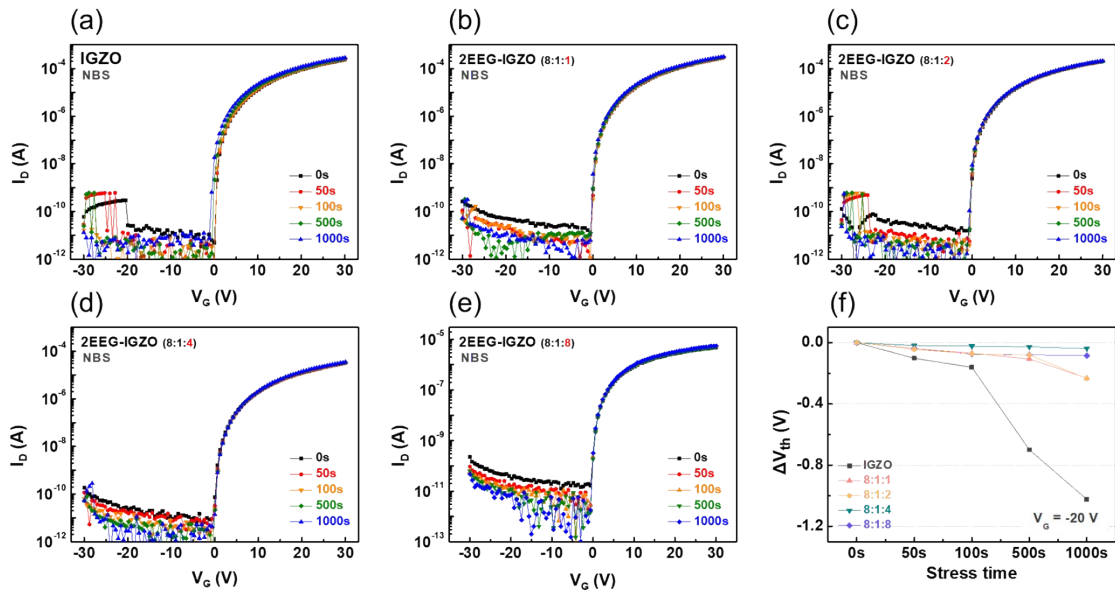


Figure S6. Transfer characteristics under NBS ($V_G = -20$ V) of (a) pristine IGZO and 2EEG-IGZOs with different volume ratios of (b) 8:1:1, (c) 8:1:2, (d) 8:1:4, and (e) 8:1:8, respectively. (f) V_{th} shift with varying stress time under NBS condition.

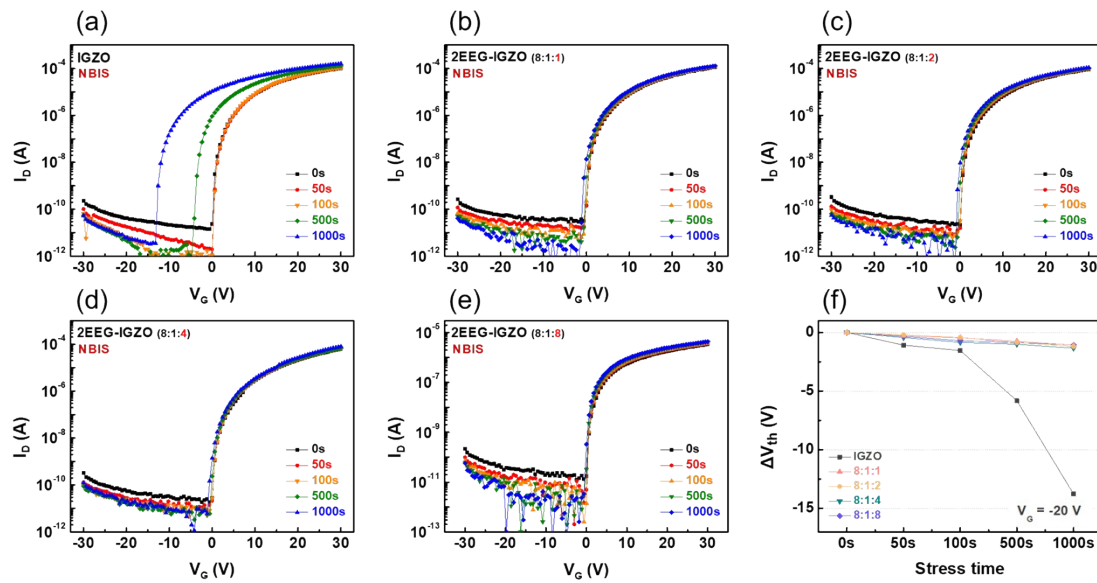


Figure S7. Transfer curves under NBIS ($V_G = -20$ V) of (a) pristine IGZO and 2EEG-IGZOs with different volume ratios of (b) 8:1:1, (c) 8:1:2, (d) 8:1:4, and (e) 8:1:8, respectively. (f)

V_{th} shift with various stress time under NBIS condition.

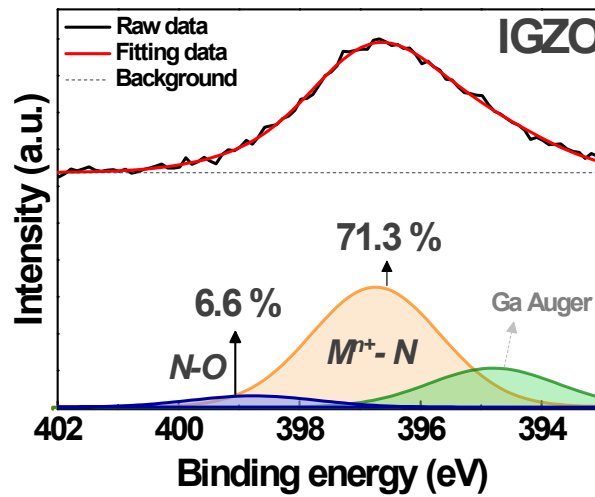


Figure S8. XPS N 1s spectra of bare IGZO sample.

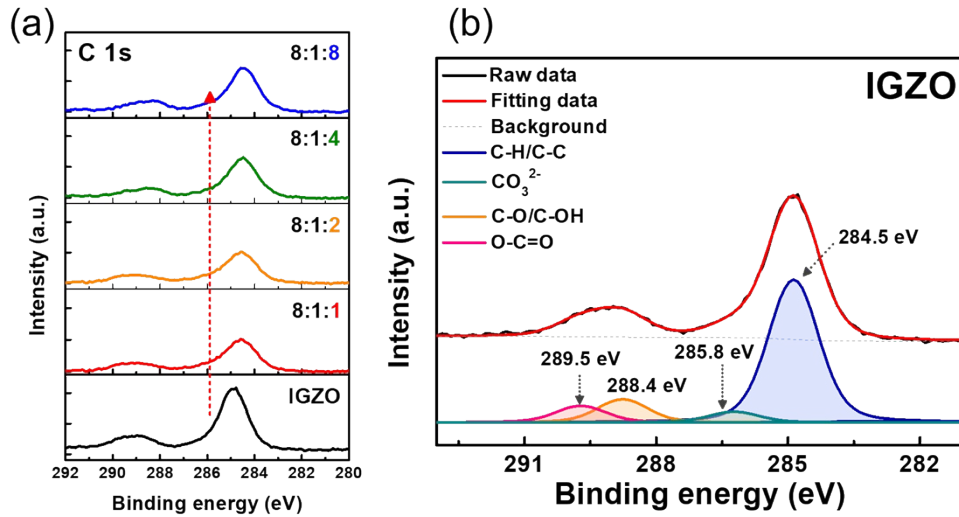


Figure S9. XPS C 1s spectra of (a) IGZO, 2EEG-IGZO samples with volume ratios of 8:1:1, 8:1:2, 8:1:4, 8:1:8 vol%, and (b) the four deconvoluted C 1s peak of IGZO.

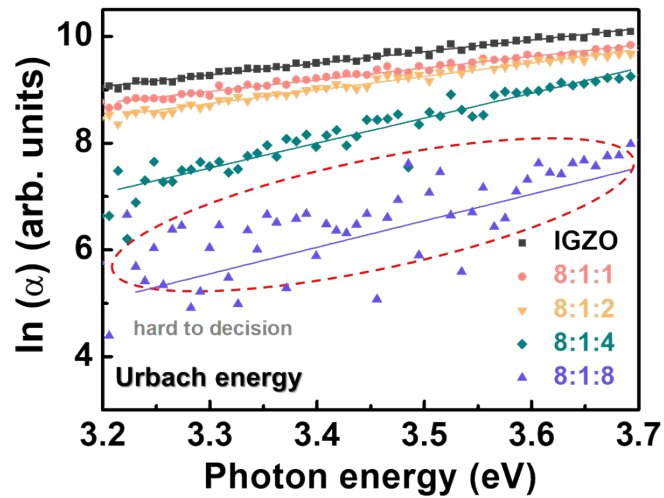


Figure S10. Urbach energy plots of the IGZO, 2EEG-IGZO samples with different additive volume ratio of 8:1:1, 8:1:2, 8:1:4, and 8:1:8 vol%, respectively.

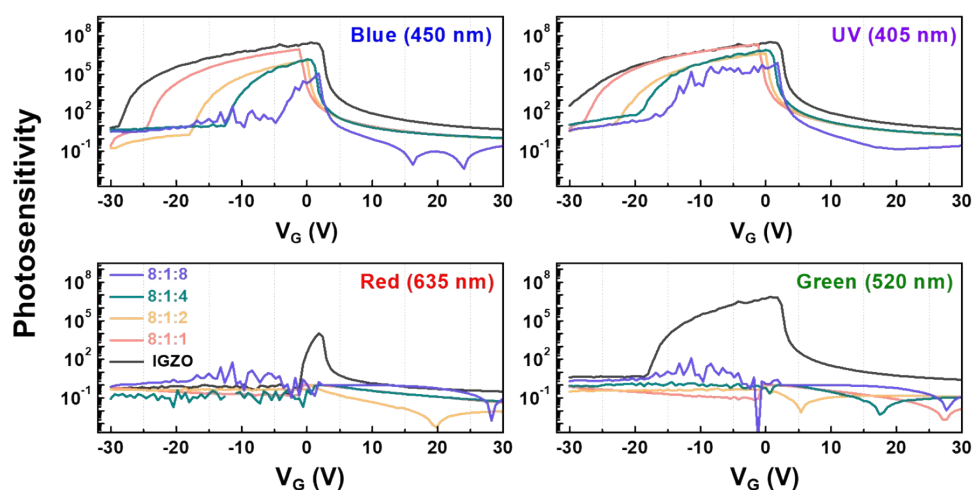


Figure S11. Photosensitivities of pristine IGZO and 2EEG-IGZO samples with varying vol% ratios (8:1:1, 8:1:2, 8:1:4, and 8:1:8) as a function of V_G , measured under red, green, blue, and UV light.

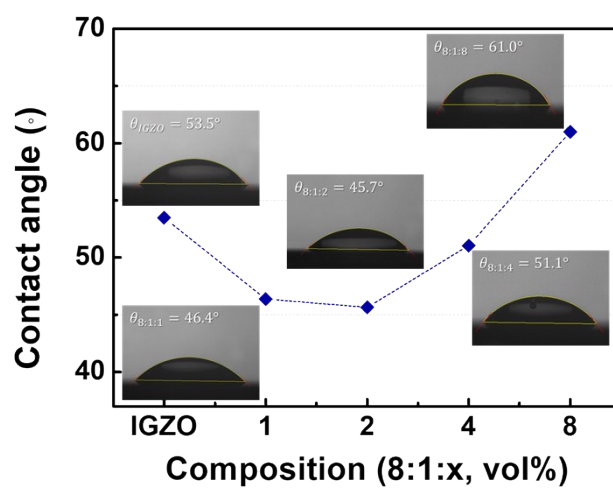


Figure S12. Contact angle measurements of IGZO and 2EEG-IGZO with various composition ratios (8:1: x).

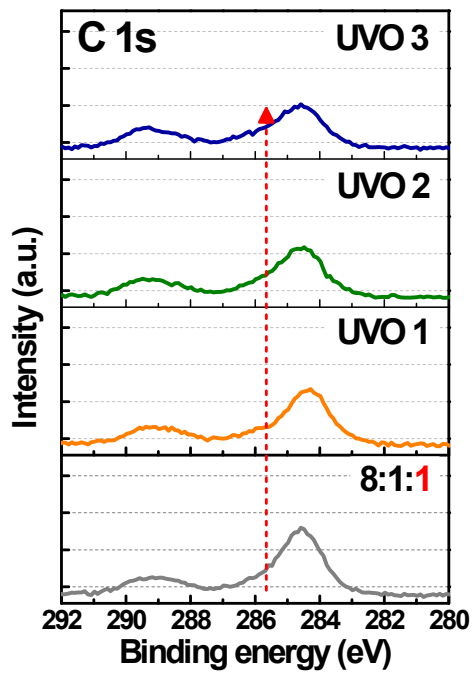


Figure S13. XPS C 1s spectra of 2EEG-IGZO samples (8:1:1 vol% ratio) without UVO treatment and with UVO treatment durations of 1 min, 2 min, and 3 min, respectively.

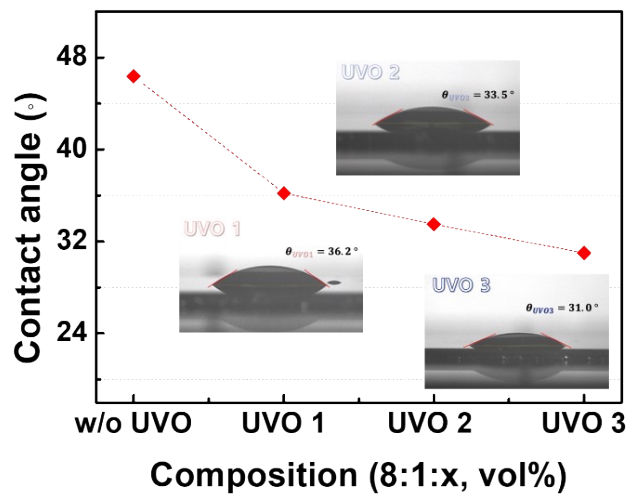


Figure S14. Contact angle measurements of 2EEG-IGZO (8:1:1 vol%) with different UVO treatment duration of 1 min, 2 min, and 3 min, respectively.

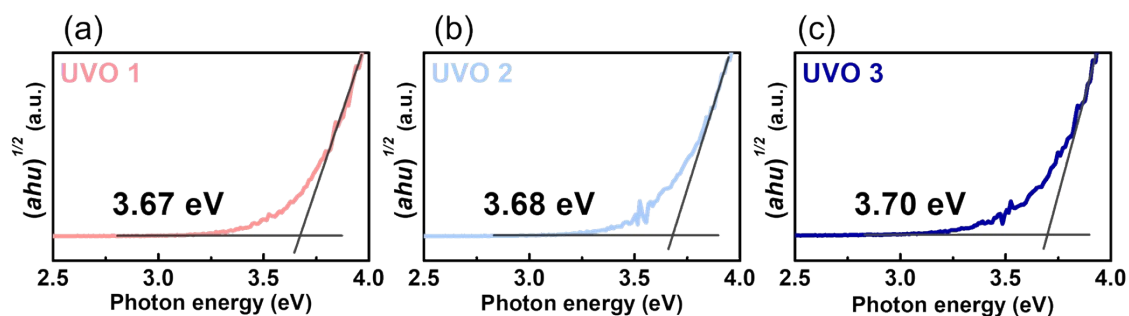


Figure S15. Optical bandgap energy of 2EEG-IGZO (8:1:1 vol% ratio) with varying UVO treatment durations: (a) 1 min, (b) 2 min, and (c) 3 min, respectively.

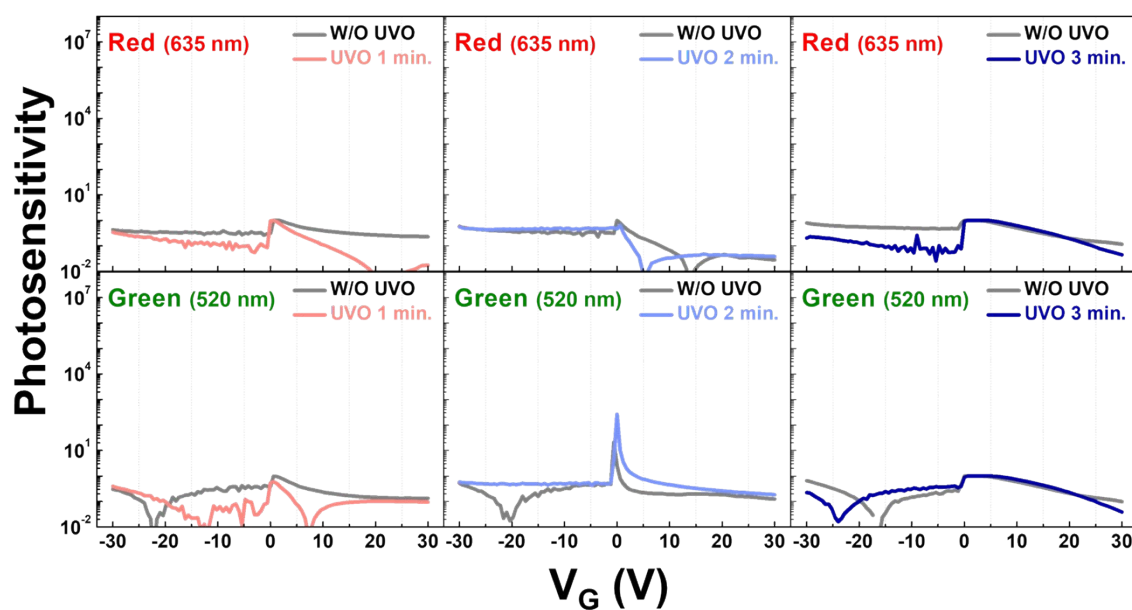


Figure S16. Photosensitivity of 2EEG-IGZO phototransistors under red (635 nm) and green (520 nm) illumination as a function of UVO treatment time.

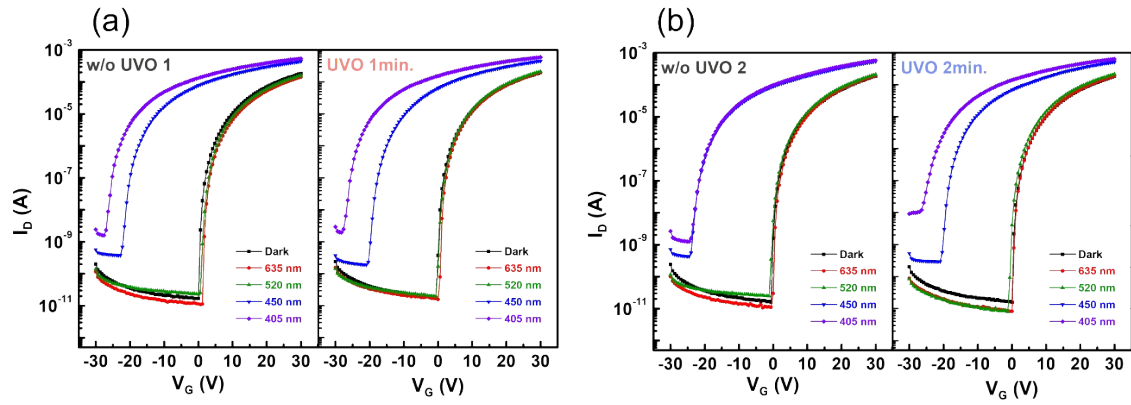
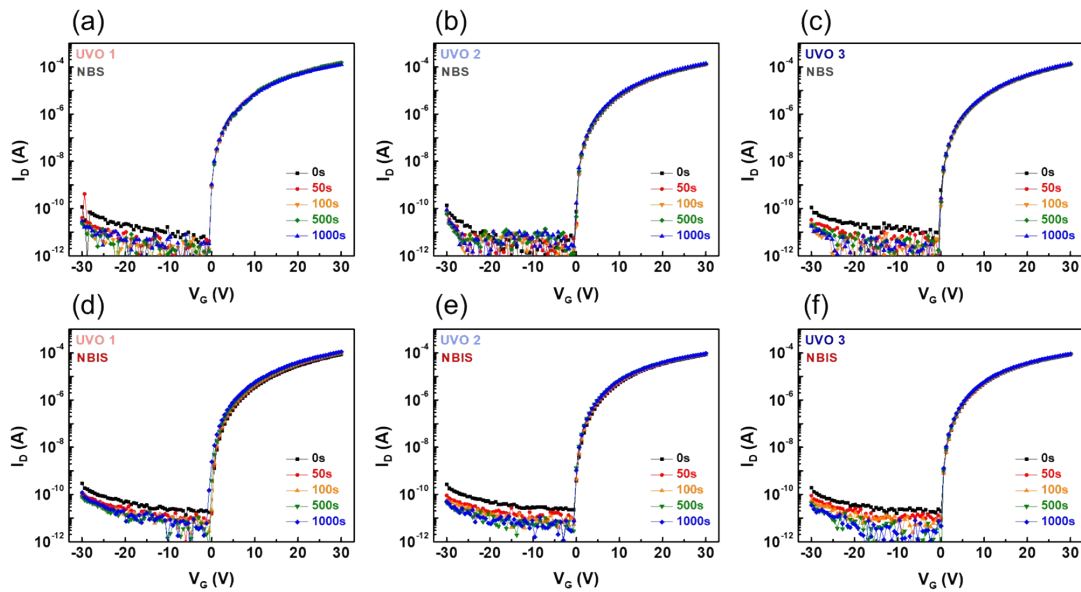


Figure S17. Photoreponse characteristics of 2EEG-IGZO phototransistors under red (635 nm) and green (520 nm) illumination as a function of UVO treatment time: (a) before (left) and after 1 min. UVO treatment (right), and (b) before (left) and after UVO treatment with a duration of 2 min.



Figure

S18. Transfer characteristics of 2EEG-IGZO (8:1:1) under NBS condition with different UVO treatment duration of (a) 1 min, (b) 2 min, and (c) 3 min, and under NBIS condition with (d) 1 min, (e) 2 min, and (f) 3 min of UVO treatment durations, respectively. ($V_G = -20V$)

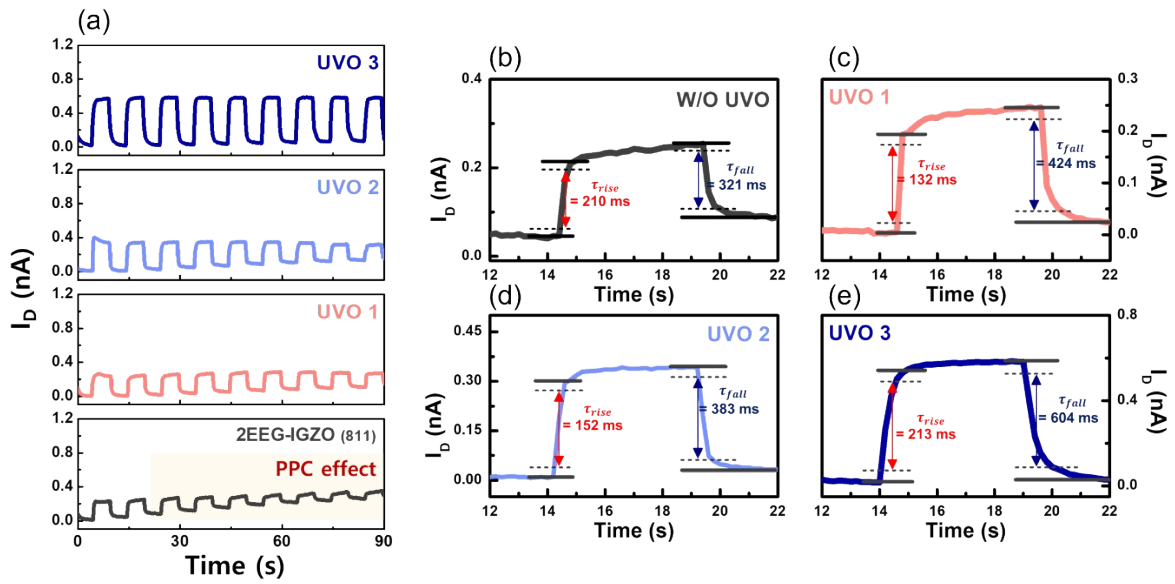


Figure S19. (a) Temporal photoresponse of 2EEG-IGZO (8:1:1 vol%) as a function of UVO treatment duration (0, 1, 2, 3 min) and (b)-(e) the corresponding rising/falling times of each sample. ($V_G = -15V$, $V_D = 0.1 V$)

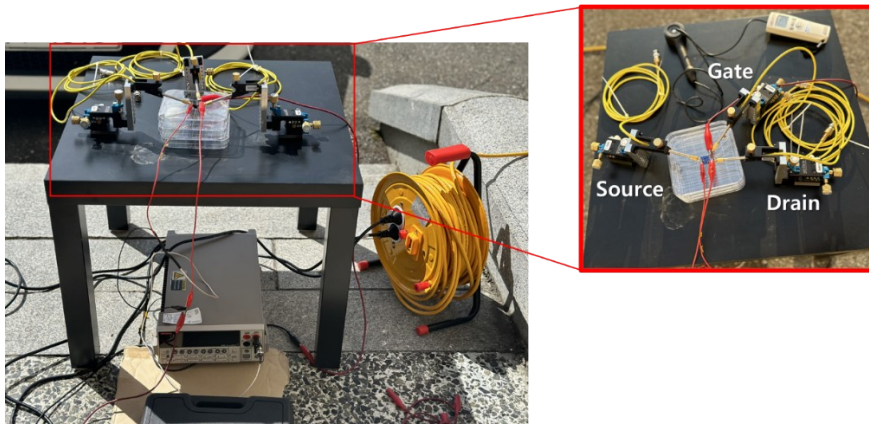


Figure S20. A real outdoor experiment image to clarify the potential of optimized 2EEG-IGZO TFTs as a real UV sensor.